Location-Aware Energy Efficient Virtual Network Embedding in Software Defined Optical Data Center Networks

Y. Zong, Y. Ou, A. Hammad, K. Kondepu, R. Nejabati, Y. Liu, L. Guo, D. Simeonidou

***Abstract*—To overcome the Internet ossification, network virtualization has been proposed as a promising method because of its advantages (e.g., on demand and efficient resource allocation). Virtual network embedding (VNE) is one of the main challenges for network virtualization. Energy costs of servers in data centers (DCs) are major contribution to power consumption in information and communication technology (ICT). Therefore, VNE should consider both acceptance ratio and power consumption. In this paper, a mixed integer linear programming (MILP) model is proposed with the objective of minimizing the total power consumption in software defined optical data center networks (SD-ODCNs) by reducing the active data centers and power-consuming network components. In addition, the coordinates of nodes and delay of links are considered for more realistic scenario. Comparing with existing node ranking method, proposed global topology resource (GTR) can effectively evaluate the possibility of each DC node to host virtual nodes. Based on GTR method, we propose location aware energy efficient VNE algorithm, namely GTR-VNE. Simulation results show that GTR-VNE can obtain up to 9.3% and 5% improvement of power consumption and acceptance ratio compared with benchmarks. Furthermore, based on GTR and artificial intelligence ant colony optimization (ACO), another energy efficient algorithm ACO-VNE is proposed. ACO-VNE can obtain up to 28.7% improvement on power consumption compared with GTR-VNE. In addition, ACO-VNE has better performance in terms of revenue cost ratio and acceptance ratio.**

***Index Terms*—Ant Colony Optimization, Energy Efficiency, Software Defined Optical Data Center Networks, Virtual Network Embedding.**

I. Introduction

THE exponential growth of dynamic high-bandwidth applications (e.g., high-definition video streaming and cloud services) increases the burden on optical data center networks (ODCNs). The traditional network architectures suffer from ossification and difficulty in supporting these types of heterogeneous and dynamic applications. To overcome the ossification, network virtualization is considered as the primary resource management paradigm for efficient resource allocation and management [1] [2]. Network virtualization enables multiple heterogeneous virtual networks (VNs) to coexist and share the resources of the substrate network (SN). Two roles and functionalities have been identified in the network virtualization environment: infrastructure provider (InP) and service provider (SP) [3]. A VN created by one or multiple SPs according to the user request is composed of a set of virtual nodes interconnected by virtual links [4]. SPs lease resources (e.g., CPU, storage and bandwidth) [5] from one or several InPs and deploy various protocols for VNs without significant investment in their own computing and network infrastructures.

However, allocating resources for both virtual nodes and links in ODCNs is a major challenge which is referred as virtual network embedding (VNE) [6]–[8]. Moreover, VNE can be divided into two sub-problems: virtual node embedding (VNoE) and virtual link embedding (VLiE). Virtual nodes can be either embedded into network devices or servers in data center (DC), and virtual links that interconnect these virtual nodes are required to be mapped onto the paths in SNs. Furthermore, delay is one of the critical quality of service (QoS) parameters, which needs to be considered to map VN requests specifically for delay-sensitive applications.

Energy consumption of SNs that provides resources is a challenge, especially for data centers [9]–[11]. Authors in [11] have proposed energy efficient MILP and VNE algorithm to minimize the power consumption by considering both node location and DC-level energy saving for ODCNs. Substrate node is selected according the residual CPU resource in this two-stage algorithm. However, the node with sufficient computing resource but insufficient bandwidth can be selected. This may cause the embedding failure. Therefore, many topology aware node ranking methods are proposed to solve this problem.

To satisfy various QoS requirements of dynamic demands, flexible network infrastructure and technologies are required to achieve the flexible and efficient service provisioning in ODCNs. To enhance the flexibility and service provisioning, DC as a service architecture has been proposed for the coordinated virtualization of optical network and computing resources of distributed DCs [12]. In [13], software-defined networking (SDN) has been introduced to provide network flexibility, where control plane enables network configuration remotely from network controller. Therefore, SDN can provide a closer tie between application requirements and the combination of resources (e.g., optical transport network, IP layer, computing and storage) [14].

Software defined data center networks have been proposed and demonstrated to achieve virtualization [15] [16]. Software

Y. Zong (e-mail: zongyue@stumail.neu.edu.cn) is with the School of Computer Science and Engineering, Northeastern University, Shenyang, China, and she is a visiting Ph.D. student with High Performance Networks Group (HPN), University of Bristol, UK.

Y. Liu (e-mail: liuyejun@cse.neu.edu.cn), L. Guo are with the School of Computer Science and Engineering, Northeastern University, Shenyang, China.

Y. Ou, A. Hammad, K. Kondepu, R. Nejabati, D. Simeonidou are with High Performance Networks Group (HPN), University of Bristol, UK.

link transceiver has been proposed for optical network device virtualization [17]. Furthermore, software defined optical data center networks (SD-ODCNs) are proposed as a promising infrastructure architecture to provide flexible virtualization to cope with dynamic requirements [18]–[20].

In this paper, we focus on energy efficient VNE in SD-ODCN by calculating the power consumption of network components and servers. Inspired by [11], a mixed integer linear programming (MILP) model is proposed to minimize the total power consumption for both DCs and the network interconnecting DCs in SD-ODCNs. A global topology resource (GTR) node ranking method is proposed to measure the possibility of each node to host virtual nodes efficiently. Based on GTR, we further propose two location aware energy efficient VNE algorithms: GTR-VNE and ACO-VNE based on the artificial intelligence (AI) ant colony optimization(ACO).

The contributions of this paper are summarized as follows:

- We propose a SD-ODCNs architecture to obtain the whole topology information in control plane and to satisfy the VNE resource requirements.
- We propose a mathematical model to formulate the power consumption by considering traffic grooming and DC-level energy saving in SD-ODCNs.
- We propose an efficient GTR node ranking method to reflect the selection possibility of each physical node. Furthermore, we propose two VNE algorithms based on GTR ranking to improve the performance in the scalability of requests and topology.

The rest of this paper is organized as follows. Section II provides an overview of related works. Section III describes software defined optical data center networks architecture. In Section IV, network model and MILP are proposed. In Section V, our proposed coordination algorithms for VNE is introduced. Simulation results and discussions are presented in Section VI. Finally, Section VII concludes this paper.

II. Related Work

VNE has been an important research topic studied for different networks in the past years, and many of the proposed approaches restrict the solution space in order to reduce its complexity. Energy efficiency in both DC networks and optical transport networks has been extensively investigated due to its importance. There are two main categories of VNE approaches: (1) independent two-stage mapping and (2) coordinated mapping. In the following section, we briefly introduce some typical and related literatures.

A. Energy Efficiency

For optical network, authors in [21]–[23] have analyzed different energy consumption models of network devices and classified the different energy-aware approaches (i.e., energy-efficient network design and green routing). Bypass and traffic grooming techniques are used for energy saving in [24] [25]. Delay performance has been considered and improved in [25] and a reconfiguration algorithm has been proposed to calculate individual dynamic high thresholds by using the output of load prediction module in [26].

For DC network, U.S. DCs are predicted to consume approximately 73 billion kWh in 2020 according to current trend [27]. Therefore, many researchers have focused on DC energy efficiency. In [28], a comprehensive survey has been discussed about energy consuming components, modeling and prediction for DCs. The architectural evolution of DCNs and their energy efficiency have been discussed in [29], with existing techniques in energy saving, green DCs and renewable energy approaches.

For ODCNs, authors have proposed a polynomial-time energy-aware routing algorithm which brings more energy saving in comparison to a shortest path-based routing algorithm and traffic grooming algorithm in [30].

B. Virtual Network Embedding

Many two-stage VNE algorithms with topology aware node ranking methods based on topological attributes (CPU of nodes and bandwidth of links)have been proposed in [31]–[34], to increase the acceptance ratio of incoming VN requests and the overall revenue of the SN. According to the ranking method by considering the resource status of nodes proposed in [31], the node with large computing resources and insufficient bandwidth still can be selected. Therefore, Markov chain-based node ranking methods are proposed by authors in [32] [33]. To quantify the embedding potential of each substrate node, proposed global resource capacity node ranking method [34] can obtain efficient ranking values. However, the existing topology aware node ranking methods have their local consideration of attributes and limitation. In addition, node location and delay are not considered.

For coordinated VNE, authors have proposed coordinated VNE algorithms using deterministic and randomized rounding techniques with better acceptance ratio comparing with two-stage VNE in [35]. Authors have proposed ILP and coordinated backtracking heuristic considering location and delay characteristic of VN for different objectives: minimizing the allocated resources and load balancing [36]. Furthermore, intelligent VNE algorithms have been proposed by using AI algorithm like ACO [37]–[39]. To satisfy the QoS requirement, VNE algorithms based on ACO have been proposed in [37] [38]. The ants move to find optimal solution through updating the cost based on the feedback information. An intelligent VNE algorithm based on genetic algorithm has been proposed in [39]. Computational effectiveness of different AI techniques and comparative performance analysis on various metrics (i.e., acceptance ratio, long-term revenue and cost) have been discussed.

C. Energy Efficient Virtual Network Embedding

Many energy efficient VNE algorithms have been proposed in [40] [41]with different optimization perspectives such as: minimizing the energy consumption or accommodating more VN requests. In [41], authors have designed an energy cost model and two VNE algorithms while maximizing the revenue.

III. Network Architecture

In this paper, we propose SD-ODCNs architecture as shown in Fig. 1 which is composed of three layers: 1) physical

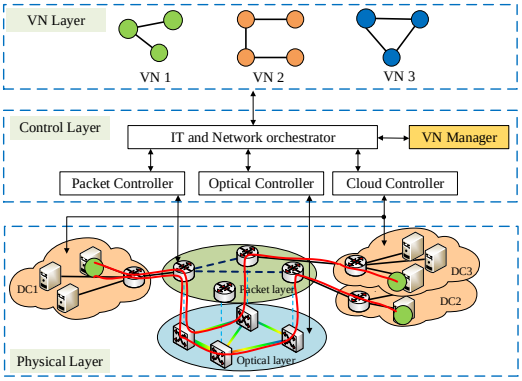

Fig. 1. SD-ODCNs Architecture. VN, virtual network; DC, data center.

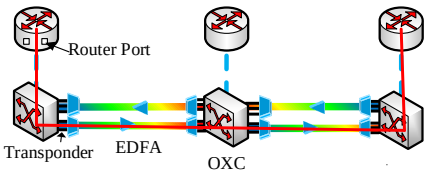

Fig. 2. Power consumption components of network. OXC: optical cross connect.

layer, 2) control layer and 3) VN layer. For physical layer, multiple geographically distributed DCs are interconnected by multi-domain networks to accommodate VN requests of VN layer. Multiple VNs are running in parallel by sharing the underlying substrate infrastructure and the coexistence and isolation of resources are ensured. Control layer provides a closer tie between VN layer and physical layer. IT and Network orchestrator can obtain the topology information from different domain controllers. The VN manager executes VNE algorithm when it receives VNs and topology information from the orchestrator. Virtual nodes should be mapped onto servers in different DCs for computing requirements. Virtual links can be embedded onto physical path in optical layer or in packet layer to satisfy the network requirements. The output results are sent from the orchestrator to different domain controllers to configure the computing and network resources.

We adopt the transparent multi-domain networks aggregation with optical network and packet network for virtual link embedding. The power consumption components of network are shown in Fig. 2. Router ports (residing in the line card) mainly dealing with electronic processing are the major energy consuming components in packet layer. In optical layer, erbium-doped fiber amplifiers (EDFAs) are equipped between optical cross connects (OXCs) which are interconnected by bi-directional fiber links. Transponders consume power due to optical-electrical-optical (OEO) conversion between the OXC and IP router. These are the main power consuming components in optical layers. In addition, servers of DC are considered as the primary power consuming components for computing resources.

IV. Network Model and Problem Description

To address the VNE problem according to the architecture shown in Fig. 1, two proposed VNE strategies are clarified by a generic logic VNE block shown in Fig. 3. Substrate network status, power consumption of components and virtual network requests are different types of input for both strategies. In addition, other major blocks for MILP are variables, objective and constraints. GTR is a node ranking method use to evaluate the selection possibility of each physical node. Based on GTR, two energy efficient VNE algorithms are proposed in section V including two sub-algorithms: virtual node embedding (VNoE) and virtual link embedding (VLiE) with the consideration of delay constraint.

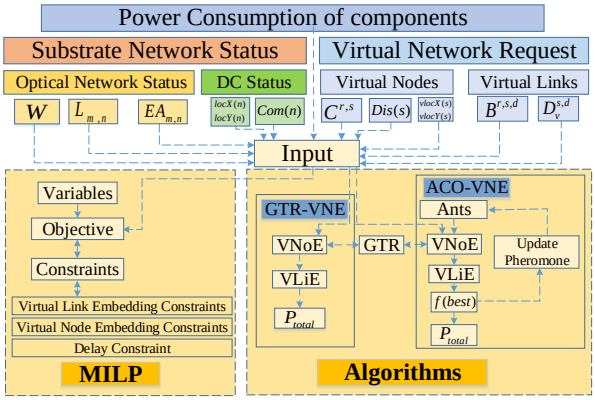

Fig. 3. Generic Logic VNE Block. GTR, global topology resource node ranking; VNoE, virtual node embedding; VLiE, virtual link embedding.

A. Substrate Network

The substrate SD-ODCNs are modeled as an undirected graph $G = (N, E)$, where $N = \{1, \cdots, n\}$ represents the set of nodes (including DC, router and optical switch node), and E represents the set of fiber links, $(m, n) \in E$. N_m is the set of adjacent nodes to node m. Each DC node n is defined with its own limited computing resource $Com(n)$ and location with coordinates $(locX(n), locY(n))$. W is the number of wavelengths in each fiber link and C is the capacity of per wavelength. $L_{m,n}$ is the physical length of the physical link (m, n). $EA_{m,n}$ is the number of EDFAs deployed along the optical physical link (m, n), and typically $EA_{m,n} = \lfloor L_{m,n}/D - 1 \rfloor + 2$, where D is the distance between two adjacent EDFAs. In addition, for virtual topology layer, i and j are the two vertices of a virtual lightpath.

The power consumption of each router port, OXC, transponder and EDFA is described as P_r, P_o, P_t and P_e, respectively. P_{base} is the base power consumption of a DC with all servers if it is active. $\mu = P_{full} - P_{idle}$ is the power gap between the full loaded server and idle server, where P_{full} and P_{idle} are the power when the server is fully loaded or idle.

B. Virtual Network

For virtual network, the undirected graph $G_v^r = (N_v^r, E_v^r)$ denotes the r^{th} virtual network request where $r \in R$, N_v^r is the set of virtual nodes and E_v^r is the set of virtual links, $(s, d) \in E_v^r$. $N_v^{r,s}$ is the set of adjacent virtual nodes to virtual node s in N_v^r. The computing resource requirement (the number of servers) of virtual node s in N_v^r is $c^{r,s}$. The location of virtual node s is $vlocX(s)$ and $vlocY(s)$. $Dis(s)$ is the acceptable maximum distance between a virtual node s and its hosting physical node. $D_v^{s,d}$ is the acceptable maximum distance which

also represents delay for virtual link (s,d). And $B^{r,s,d}$ is the bandwidth requirement of the virtual link in E_v^r.

C. Variables Definition

There are many variables defined as follows:

1) Binary Variables:

- $\sigma_n^{r,s}$: If virtual node s of N_v^r is mapped into the physical node n, $\sigma_n^{r,s}=1$; otherwise, $\sigma_n^{r,s}=0$.
- $\vartheta^{s,d,i,j}$: If virtual link (s,d) is mapped onto lightpath (i,j) in virtual topology, $\vartheta^{s,d,i,j}=1$, otherwise, $\vartheta^{s,d,i,j}=0$.
- $\xi_{m,n}^{i,j}$: If lightpath (i,j) is mapped onto physical link (m,n), $\xi_{m,n}^{i,j}=1$, otherwise, $\xi_{m,n}^{i,j}=0$.
- $\chi_{m,n}^{s,d,i,j}$: If virtual link (s,d) is mapped onto lightpath (i,j) and lightpath (i,j) is mapped onto physical link (m,n), $\chi_{m,n}^{s,d,i,j}=1$, otherwise, $\chi_{m,n}^{s,d,i,j}=0$.
- δ_n: If DC node n is active $\delta_n=1$, otherwise, $\delta_n=0$.
- Φ_n^r: if DC node n is mapped by any virtual node of r^{th} VN request $\Phi_n^r=1$, otherwise, $\Phi_n^r=0$.

2) Integral Variables:

- $\omega_{m,n}$: Number of wavelength channels in the physical link (m,n).
- $\theta^{i,j}$: Number of wavelength channels in the lightpath (i,j).
- $\eta_{m,n}^{i,j}$: Number of wavelength channels in the lightpath (i,j) traversing over the physical link (m,n).

D. Objective

Our objective is to minimize the total power consumption (including network and DC power consumption) of SD-ODCNs as shown in Eq. 1. The power consumption of network is shown in Eq. 2, which is the sum of power consumption of various components such as router ports, transponders, EDFAs. Equation 3 is the power consumption of DCs (as we just consider the power consumption of servers) considering sleep mode for unused servers if the DC node is active.

$$Minimize: \qquad P_{total}=P_{net}+P_{dc}, \tag{1}$$

$$\begin{aligned} P_{net} &= \sum_{m\in N}\sum_{n\in N_m}(P_t\cdot\omega_{m,n}+P_e\cdot EA_{m,n})+ \\ &\sum_{i\in N}\sum_{j\in N:j\neq i}P_r\cdot\theta^{i,j}+\sum_{m\in N}P_o, \end{aligned} \tag{2}$$

$$P_{dc}=\sum_{n\in N}\sum_{r\in R}\sum_{s\in N_v^r}c^{r,s}\cdot\sigma_n^{r,s}\cdot\mu+\sum_{n\in N}\delta_n\cdot P_{base}, \tag{3}$$

E. Constraints

1) Virtual Node Embedding Constraints: Equations 4-9 are virtual node embedding constraints. Equation 4 guarantees that a DC node should provide adequate computing resource for all virtual nodes that are accommodated by this DC node, where $\sigma_n^{r,s}$=1, if virtual node s of VN r is mapped into the physical node n. In Eq. 5, each virtual node s can be only hosted once by a unique DC node. DC node can only host one virtual node of a request in Eq. 6. DC node n is active if it is used to host any VN request shown in Eq. 7, where $\Phi_n^r=\sum_{s\in N_v^r}\sigma_n^{r,s}$. The distance constraints for virtual nodes are shown in Eqs. 8-9.

$$\sum_{r\in R}\sum_{s\in N_v^r}c^{r,s}\cdot\sigma_n^{r,s}\leq Com(n),\forall\ n\in N, \tag{4}$$

$$\sum_{n\in N}\sigma_n^{r,s}=1,\quad \forall r\in R, s\in N_v^r, \tag{5}$$

$$\sum_{s\in N_v^r}\sigma_n^{r,s}\ \leq 1,\ \forall n\in N, r\in R, \tag{6}$$

$$\delta_n=\prod_{r\in R}\Phi_n^r, \forall n\in N, \tag{7}$$

$$\begin{aligned} &\sigma_n^{r,s}abs(vlocX(s)-locX(n))\leq Dis(s), \\ &\forall n\in N, r\in R, s\in N_v^r, \end{aligned} \tag{8}$$

$$\begin{aligned} &\sigma_n^{r,s}abs(vlocY(s)-locY(n))\leq Dis(s), \\ &\forall n\in N, r\in R, s\in N_v^r, \end{aligned} \tag{9}$$

2) Virtual Link Embedding Constraints: Virtual link embedding constraints are shown in Eqs. 10-17. Total carried bandwidth resource requirement can not exceed occupied wavelength capacity on lightpath (i,j) is ensured by Eq. 10. Equation 11 represents the flow conservation constraint for optical layer. Equation 12 is used to find the shortest path on optical layer for lightpath (i,j). Equations 13-15 ensure that the sum of all traffic flows through an optical link (m,n) does not exceed its capacity. The variable $\vartheta^{s,d,i,j}$ in Eq. 14 is required for variable $\chi_{m,n}^{s,d,i,j}$ in Eq. 15, which is used in Eq. 13. Equation 16 ensures that the number of allocated wavelengths cannot exceed the initial capacity of an optical link. The total number of occupied wavelength channels for an optical link is shown in Eq. 17.

$$\sum_{r\in R}\sum_{s\in N_v^r}\sum_{d\in N_v^{r,s}}\vartheta^{s,d,i,j}\cdot B^{r,s,d}\leq\theta^{i,j}\cdot C, \forall i,j\in N, i\neq j, \tag{10}$$

$$\begin{aligned} &\sum_{n\in N_m}\eta_{m,n}^{i,j}-\sum_{n\in N_m}\eta_{n,m}^{i,j}=\begin{cases}\theta^{i,j}, & if\ m=i\\ -\theta^{i,j}, & if\ m=j\\ 0, & others\end{cases} \\ &\forall i,j,m\in N, i\neq j, \end{aligned} \tag{11}$$

$$\begin{aligned} &\sum_{n\in N_m}\xi_{m,n}^{i,j}-\sum_{n\in N_m}\xi_{n,m}^{i,j}=\begin{cases}1, & if\ \ m=i\\ -1, & if\ \ m=j\\ 0, & others\end{cases} \\ &\forall i,j,m\in N, i\neq j, \end{aligned} \tag{12}$$

$$\begin{aligned} &\sum_{r\in R}\sum_{s\in N_v^r}\sum_{d\in N_v^{r,s}}\chi_{m,n}^{s,d,i,j}\cdot B^{r,s,d}\leq\eta_{m,n}^{i,j}\cdot C, \\ &\forall m,i,j\in N, n\in N_m, \end{aligned} \tag{13}$$

$$\vartheta^{s,d,i,j}=\sigma_i^{r,s}\cdot\sigma_j^{r,d}, \tag{14}$$

$$\chi_{m,n}^{s,d,i,j}=\vartheta^{s,d,i,j}\cdot\xi_{m,n}^{i,j}, \tag{15}$$

$$\sum_{i\in N}\sum_{j\in N:i\neq j}\eta_{m,n}^{i,j}\leq W,\ \forall m\in N, n\in N_m, \tag{16}$$

$$\sum_{i\in N}\sum_{j\in N:i\neq j}\eta_{m,n}^{i,j}=\omega_{m,n}, \forall m\in N, n\in N_m, \tag{17}$$

3) Delay Constraint: Equation 18 is the delay constraint to ensure that the path transmission delay does not exceed the maximum acceptable delay for virtual link (s,d) in r^{th} VN request. For simplicity, path length represents the transmission delay since the delay of the physical link (m,n) is $D_{m,n}$ =$L_{m,n}/c$, where, $c = 2 \times 10^5 km/s$ is the speed of signal in fiber [42]. In addition, delay can be obtained from the SDN controller.

$$\sum_{m\in N}\sum_{n\in N_m} \chi_{m,n}^{s,d,i,j} \cdot L_{m,n} \le D_v^{s,d}, \quad \forall i,j \in N, i \ne j, r \in R, s \in N_v^r, d \in N_v^{r,s}. \tag{18}$$

F. Linearization

The problem described above is a mixed integer quadratically constrained program (MIQCP) because Eqs. 7, 14 and 15 contain quadratic term variables δ_n, $\vartheta^{s,d,i,j}$ and $\chi_{m,n}^{s,d,i,j}$. In this section, to decrease the complexity of the model, nonlinear equations are linearized by the following constraints, where ε is a maximum positive integer constant.

$$(\sum_{r\in R}\Phi_n^r)/\varepsilon \le \delta_n \le (\sum_{r\in R}\Phi_n^r)\cdot\varepsilon, \tag{19}$$

$$0 \le \vartheta^{s,d,i,j} \le \sigma_i^{r,s}, \tag{20}$$

$$\sigma_i^{r,s} + \sigma_j^{r,d} - 1 \le \vartheta^{s,d,i,j} \le \sigma_j^{r,d}, \tag{21}$$

$$0 \le \chi_{m,n}^{s,d,i,j} \le \vartheta^{s,d,i,j}, \tag{22}$$

$$\vartheta^{s,d,i,j} + \xi_{m,n}^{i,j} - 1 \le \chi_{m,n}^{s,d,i,j} \le \xi_{m,n}^{i,j}. \tag{23}$$

Therefore, the MIQCP problem is linearized into a MILP model as follows:

Minimize: (1)
s.t. (2)-(6),
(8)-(13),
(16)-(23).

V. Energy Efficient Virtual Network Embedding Algorithm

According to the MILP proposed in the above section, the VNE problem can not be solved in polynomial-time when network topology scales. To overcome this issue, two VNE algorithms are proposed based on GTR node ranking method by considering the topological attributes.

A. Global Topology Resource Node Ranking

First available (FA) computing resource is a typical method for virtual node embedding stage. However, the path between two high ranking value nodes may not satisfy the requirement of virtual link. Therefore, local node ranking (LNR) is proposed by considering topological attributes (i.e., available computing resource q_m and bandwidth resource $b(m,n)$) according to Eq. 24, where $l(m)$ is the ranking value. However, LNR ranking value still can cause VNE failure since it only considers the resources of the node itself. Furthermore, to evaluate the embedding potential of virtual node to each node in the substrate network, GTR ranking $g(m)$ of node m is formulated as Eq. 25, where, α is a factor and $\alpha \in (0,1)$, Q_m is the normalized computing resource of node m shown as Eq. 26, and $p(m,n)$ is the transition factor defined as Eq. 27.

$$l(m) = q_m \cdot \sum_{(m,n)\in E} b(m,n) \tag{24}$$

$$g(m) = (1-\alpha)\cdot Q_m + \alpha \cdot \sum_{n\in N_m} p(m,n)\cdot g(n), \tag{25}$$

$$Q_m = \frac{q_m}{\sum\limits_{n\in N} q_n}, m \in N, \tag{26}$$

$$p(m,n) = \begin{cases} \frac{b(m,n)/L_{m,n}}{\sum\limits_{x\in N} b(x,n)/L_{x,n}}, & (m,n)\in E \\ 0, & otherwise \end{cases} \tag{27}$$

GTR for all nodes can be formulated using a vector format as $\mathbf{g}$=$(1-\alpha)\mathbf{Q} + \alpha\mathbf{P}\mathbf{g}$, where, $\mathbf{g}$=$(g(1), g(2), ..., g(|N|))^T$, $\mathbf{Q}$=$(Q_1, Q_2, ...Q_{|N|})^T$, and $\mathbf{P}$ is a transition matrix with dimension as $|N| \times |N|$. For transition matrix, we consider both the available bandwidth and delay as defined in Eq. 27. Therefore, an iteration algorithm is used to calculate the GTR vector as $\mathbf{g}_{k+1}$=$(1-\alpha)\mathbf{Q}+\alpha\mathbf{P}\mathbf{g}_k$, where $\mathbf{g}_k$ is the vector after k iterations. A smaller threshold ϵ is designed for iteration, $\epsilon \ll 1$. Algorithm 1 shows the details of calculating vector $\mathbf{g}$, and its complexity is $O(|N|^2 \log \frac{1}{\epsilon})$.

Algorithm 1 Global Topology Resource (GTR)

Input: $G(N,E)$, ϵ,
Output: GTR vector $\mathbf{g}$,
1: Calculate $\mathbf{P}$ and $\mathbf{Q}$,
2: $\mathbf{go} = \mathbf{Q}$,
3: $k = 0$,
4: $\Delta = \infty$,
5: **while** $\Delta > \epsilon$ **do**
6: $\quad \mathbf{g}_{k+1} = (1-\alpha)\mathbf{Q} + \alpha\mathbf{P}\mathbf{g}_k$,
7: $\quad \Delta = ||\mathbf{g}_{k+1} - \mathbf{g}_k||$,
8: $\quad k = k+1$,
9: **end while**
10: $\mathbf{g} = \mathbf{g}_k$.

B. Energy Efficient Virtual Network Embedding

In this section, we propose two energy efficient VNE algorithms. The first algorithm is a two-stage VNE algorithm based on GTR node ranking (GTR-VNE) as shown in Algorithm 2. For each request r, VLiE will be executed if virtual node embedding result Em_v has been returned after executing VNoE successfully. The details of VNoE and VLiE are introduced in following parts. Total power consumption P_{total} is calculated if virtual link embedding result El_v is returned. Otherwise the request is rejected. The time complexity of GTR-VNE is $O(|R|\cdot(|N_v|^2 \log |N_v| + |E_v|\cdot|E| \log |N|))$.

The second algorithm is a coordinated virtual network embedding algorithm (ACO-VNE) based on ACO considering GTR node ranking as shown in Algorithm 3. For each request r, it initializes transition probability matrix $t_{i,j}$ and pheromone matrix $\tau_{i,j}$, where $\psi_{i,j}$ and $\Delta\tau_{i,j}$ are heuristic visibility for movement and increment of pheromone. For each ant in the set of generated ants, it executes VNoE and VLiE. Then $f(best)$ referred as optimal solution is updated by

Algorithm 2 GTR-VNE

Input: $G(N,E)$, $G_v(N_v\ E_v)$, Em_v, El_v,
Output: P_{total},
for all r $\in$ R **do**
  Execute VNoE using Algorithm 4,
  if Em_v **then**
    Execute VLiE using Algorithm 5,
    if El_v **then**
      Update P_{total},
    else
      Reject the request,
    end if
  else
    Reject the request,
  end if
end for

Algorithm 3 ACO-VNE

Input: $G(N,E)$, $G_v(N_v\ E_v)$, $\{P\}$, K,
Output: P_{total},
for all r $\in$ R **do**
  Initialize the pheromone matrix, transition probability matrix, the best ant $f(Best) = +\infty$, generate a set of ants,
  $k = 0$,
  while $k < |K|$ **do**
    for all ant **do**
      Execute VNoE using Algorithm 4,
      Execute VLiE using Algorithm 5,
    end for
    if $f(local) < f(best)$ **then**
      $f(best) \leftarrow f(local)$
    end if
    Update the pheromone,
  end while
end for

Algorithm 4 Virtual Node Embedding (VNoE)

Input: $G(N,E)$, $G_v(N_v\ E_v)$,
Output: VNoE result Em_v,
Sort all virtual nodes to $G_v(s)$ using Algorithm 1;
for all $s \in G_v(s)$ **do**
  Sort substrate nodes to $G_n(n)$ using Algorithm 1;
  Establish candidate node set $N_c(s)$;
  if $N_c(s)$!= $\varnothing$ **then**
    Choose corresponding physical node in $N_c(s)$ for each virtual node, and mark it as active;
    Update computing resource;
  else
    Reject the request;
  end if
end for

Algorithm 5 Virtual Link Embedding (VLiE)

Input: $G(N,E)$, $G_v(N_v\ E_v)$,Em_v,
Output: VLiE result El_v;
for all $(s,d) \in E_v^r$ **do**
  Establish link auxiliary graph on virtual topology layer and find the shortest path;
  if successful **then**
    Update bandwidth status;
  else
    Find the shortest path on the optical layer;
    Create a new lightpath (i,j) ;
    if successful **then**
      Update bandwidth status;
    else
      Reject the request;
    end if
  end if
end for

using fitness function if the local result $f(local) < f(best)$, where f is total power consumption. The pheromone matrix is updated according to Eq. 28-29, where β, γ and $\rho \in$ (0,1) are ACO factors. The time complexity of ACO-VNE is $O(|R| \cdot |K| \cdot |A| \cdot (|N_v|^2 \log |N_v| + |E_v| \cdot |E| \log |N|))$, where $|A|$ is the number of ants and $|K|$ is the maximum iteration number for ACO.

$$t_{i,j} = \frac{(\tau_{i,j})^{\gamma} \cdot (\psi_{i,j})^{\beta}}{\sum_{h \in N_i} (\tau_{i,h})^{\gamma} \cdot (\psi_{i,h})^{\beta}}, m \in N, \tag{28}$$

$$\tau_{i,j} = (1-\rho)\tau_{i,j} + \Delta\tau_{i,j} \tag{29}$$

1) Virtual Node Embedding (VNoE): For virtual node embedding stage, we propose VNoE based on GTR node ranking as shown in Algorithm 4. We sort the virtual nodes into $G_v(s)$ in descending order according to GTR. Then, for each virtual node s in $G_v(s)$, all substrate nodes are sorted into $G_n(n)$ in descending order according to GTR. Candidate node set $N_c(s)$ is established if the nodes in $G_n(n)$ satisfy the requirements of virtual node s such as computing and location. If there exist candidate nodes in $N_c(s)$, the first one is selected. Otherwise, the request is rejected. For each chosen DC node, it needs to be marked as active. Finally, the virtual node embedding result Em_v is returned. The time complexity is $O(|N_v|^2 \cdot \log |N_v|)$ since the time complexity of recursive function is $O(|N_v| \cdot \log |N_v|)$.

2) Virtual Link Embedding (VLiE): For virtual link embedding stage, link auxiliary graph which pre-cuts all the links without enough available bandwidth resources is established on virtual topology layer which is packet layer on the top of optical layer. Then, the shortest path satisfying the delay parameter is found by using *Dijkstra algorithm*. Otherwise, a new lightpath is established during searching for the shortest path on optical layer. If there exists available path, the bandwidth status would be updated. Otherwise, the substrate network status is reset and the VNR is rejected. The details of VLiE is shown in Algorithm 5 and the time complexity is $O(|E_v| \cdot |E| \log |N|)$.

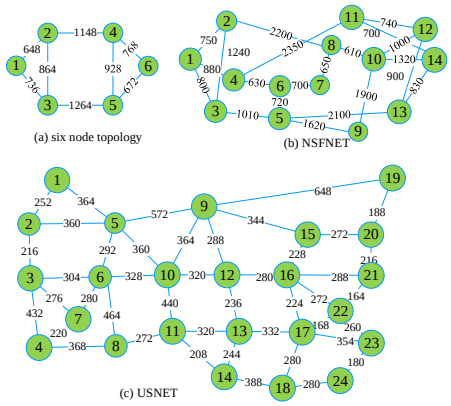

Fig. 4. Network Topologies

TABLE I
SIMULATION PARAMETERS

Parameters	Notation	Value
Distance between the adjacent EDFAs [km]	$L_{m,n}$	80
Capacity of each wavelength [Gbps]	C	40
Power consumption of a router port [kW]	P_r	1
Power consumption of a transponder [kW]	P_t	0.073
Power consumption of an EDFA [kW]	P_e	0.016
Power consumption of an optical switch [kW]	P_o	0.085
Power of full load server [kW]	P_{full}	0.365
Power of idle server [kW]	P_{idle}	0.112

VI. Simulation Results and Discussions

A. Simulation Setup

In this section, we describe the simulation environment and performance metrics used for the proposed algorithms. We evaluate the proposed MILP and algorithms in three different network topologies: (1) six-node topology (2) NSFNET and (3) USNET as shown in Fig. 4. In this figure, the number associated with each link represents the physical distance of the link (in km). The computing capacity $Com(n)$ of each data center node is uniformly distributed between 400 and 500. The number of wavelength W in a fiber is uniformly distributed between 50 and 80.

All virtual nodes and virtual links in VN requests are generated randomly. Each pair of virtual nodes is connected randomly with a probability of 0.5 to generate different virtual topologies. The number of virtual nodes for each VN is assumed to be uniformly distributed random variable over range [2, 4]. Computing resource for each virtual node is assumed the range within [1, 3] units. Bandwidth requirements of virtual links are uniformly distributed from [20, 50] Gbps. Each substrate node and virtual node is randomly located within a uniformly distributed position between 0 and 50 on x and y coordinates. We use 95% confidence interval and each scenario is performed 100 times randomly. Table I shows the simulation parameters, and the corresponding values are set as in [11].

To evaluate the performance, the following metrics are measured:

- *Acceptance Ratio*: defined as the percentage of accepted VNs to the total number of received VNs.
- *Power Consumption*: described as P_{total}, P_{dc} and P_{net} which are different power consumption values defined in Section IV-D.
- *Active DC Number*: defined as the number of active DC nodes.
- *Running Time*: defined as the average time spent by each algorithm for each VN request.
- *Revenue-Cost (R/C) Ratio*: defined as the efficiency of substrate resource usage, as shown in Eqs. 30-31.

$$\mathbb{R} = \sum_{r \in R} \Big(\sum_{s \in V_v^r} c^{r,s} + \sum_{(s,d) \in E_v^r} B^{r,s,d} \Big) \tag{30}$$

$$\mathbb{C} = \sum_{r \in R} \Big(\sum_{s \in V_v^r} c^{r,s} + \sum_{(s,d) \in E_v^r} \chi_{m,n}^{s,d,i,j} \cdot B^{r,s,d} \Big) \tag{31}$$

B. Comparisons for MILP and Algorithms

We implement MILP on ILOG CPLEX solver and algorithms using C++ on Linux operating system running in a 64-bit computer with 3.7 GHz Intel CPU and 16 GB RAM. Table II shows the comparison of power consumption for MILP and proposed algorithms. The average optimality gap of total power consumption P_{total} between proposed ACO-VNE and MILP solution can be around 6% and 7%, under six-node topology and NSFNET, respectively. The reason is that our proposed algorithms decrease the solution space by cutting some unsatisfied candidate solutions for each request.

In addition, the comparison of *Running Time* T under two different topologies is shown in Table II. Compared with the six-node topology, the *Running Time* for MILP under NSFNET increases 7 and 66 times when the number of VNs equals to 5 and 10, respectively. Moreover, MILP can not obtain the optimal solution in a reasonable time period due to high complexity when the number of VNs is 15 under NSFNET topology. As a result, the *Running Time* of the proposed algorithms is 99% less than MILP.

C. Comparisons for Algorithms in Large-scale Topologies

The FA-VNE and LNR-VNE algorithms are used as benchmarks described in Section V-A. In this section, we discuss the impact of VNs, topologies and factor value (e.g., α, β and γ) on our proposed algorithms.

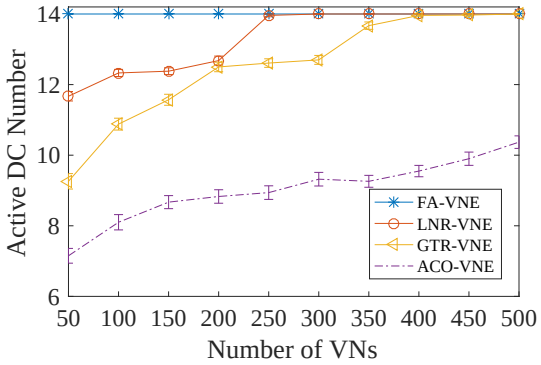

Fig. 6. Active DC Number for NSFNET

For NSFNET topology, the obtained results as a function of number of VNs are shown in Figs. 5-9. Both factor values of α and γ are set to 0.5 and β is set to 0.8. Figure 5(a)

TABLE II
COMPARISONS OF POWER CONSUMPTION AND RUNNING TIME

Number of VNs		5			10			15		
VNE Mechanism		MILP	ACO-VNE	GTR-VNE	MILP	ACO-VNE	GTR-VNE	MILP	ACO-VNE	GTR-VNE
Six-node	P_{net} [kW]	11.8	27.72	27.86	19.31	43.32	48.05	21.19	66.49	72.39
	P_{dc} [kW]	406.83	406.83	406.83	414.17	414.17	414.17	419.73	419.73	419.73
	P_{total} [kW]	418.63	434.55	434.69	433.48	462.22	462.22	451.92	486.22	492.12
	T [sec]	20.27	0.22	0.03	108.25	0.41	0.08	935.03	0.69	0.13
NSFNET	P_{net} [kW]	24.68	39.8	45.26	34.34	82.51	84.07	-	90.95	101.14
	P_{dc} [kW]	407.34	407.34	507.34	418.72	418.72	515.68	-	524.54	524.54
	P_{total} [kW]	432.02	447.13	552.6	453.06	501.23	599.76	-	523.68	523.68
	T [sec]	148.42	0.54	0.14	6680.31	1.23	0.289	-	1.65	0.42

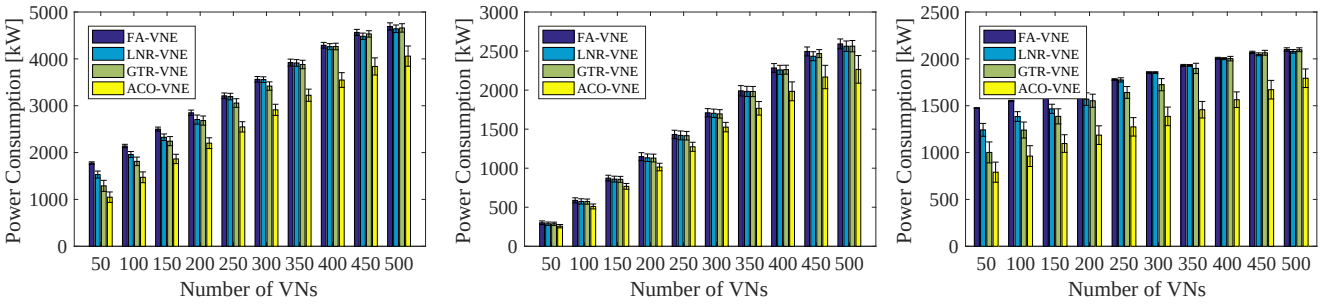

(a) Total Power Consumption (b) Network Power Consumption (c) DC Power Consumption

Fig. 5. Comparison of power consumption for NSFNET

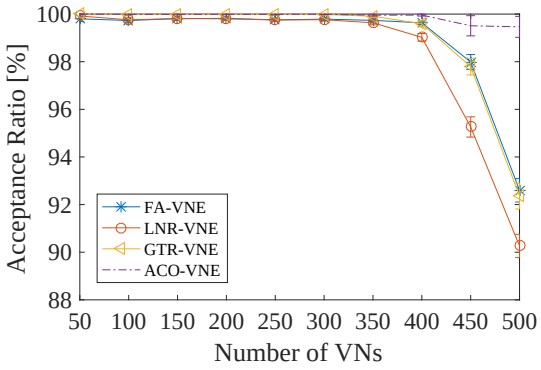

Fig. 7. Acceptance Ratio for NSFNET

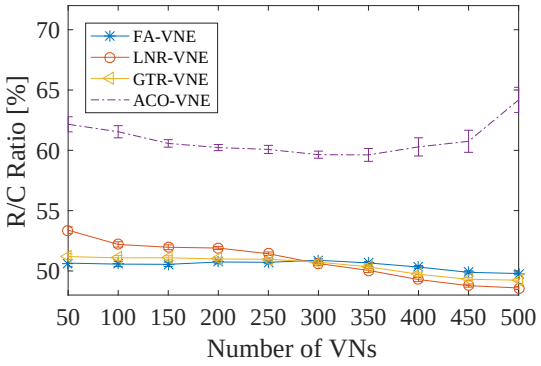

Fig. 9. Revenue-Cost Ratio for NSFNET

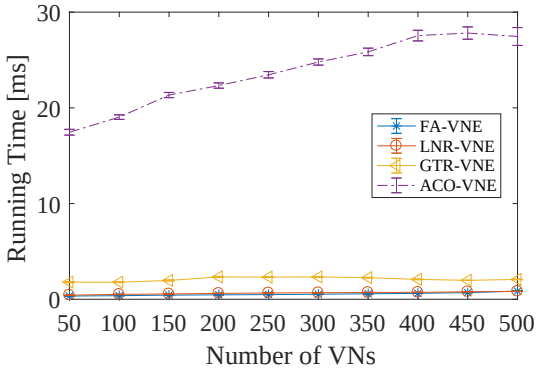

Fig. 8. Average Running Time for NSFNET

shows the average total power consumption of four different algorithms. The results of GTR-VNE obtain 9.3% and 5.1% improvement when compared with the FA-VNE and LNR-VNE. This is because the GTR node ranking helps to decrease the total power consumption. The proposed ACO-VNE further decreases the total power consumption up to 18.8% when compared with GTR-VNE. This is because ACO-VNE can choose the best solution by updating pheromone (marker) according to the candidate results. For the network power consumption P_{net} shown in Fig. 5(b), the improvement ratio of ACO-VNE is fluctuated between 10% and 14.6% compared with the other three algorithms. In Fig. 5(c), DC power consumption P_{dc} of ACO-VNE is able to reduce up to 46.4%, 36.4% and 23.6% compared to FA-VNE, LNR-VNE and GTR-VNE, respectively. In addition, the active DC number of ACO-VNE is reduced by 3 to 5 compared with other three algorithms as shown in Fig. 6.

In Fig. 7, the *Acceptance Ratio* of ACO-VNE is above 99.5%. The improvement can be up to 9.2% when the number of requests is equal to 500. The comparison of average *Running Time* for each request is shown in Fig. 8. For FA-VNE (LNR-VNE) and GTR-VNE, the average time for each

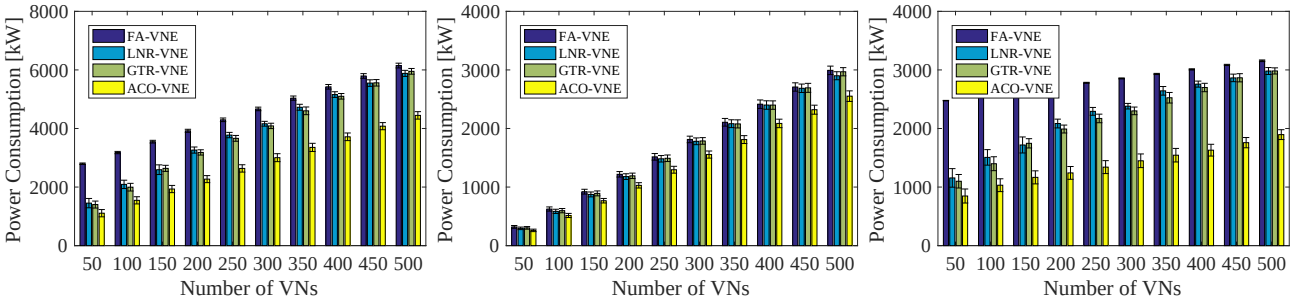

(a) Total Power Consumption (b) Network Power Consumption (c) DC Power Consumption

Fig. 10. Comparison of power consumption for USNET

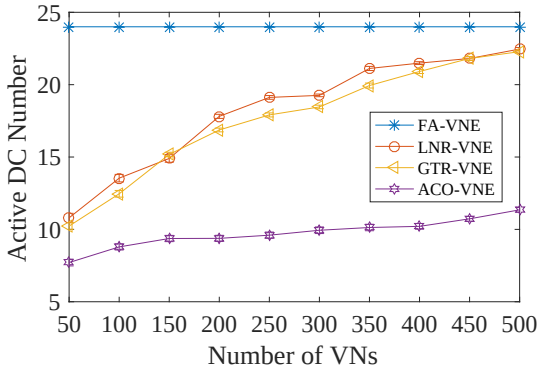

Fig. 11. Active DC Number for USNET

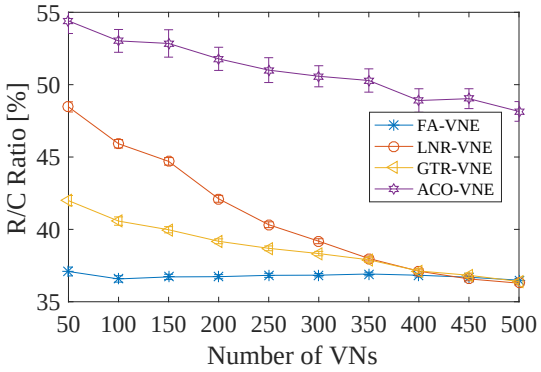

Fig. 14. Revenue-Cost ratio for USNET

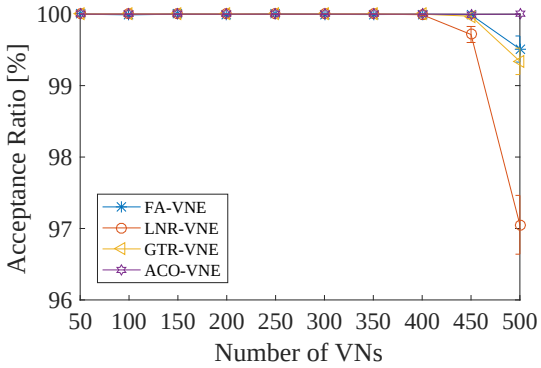

Fig. 12. Acceptance Ratio for USNET

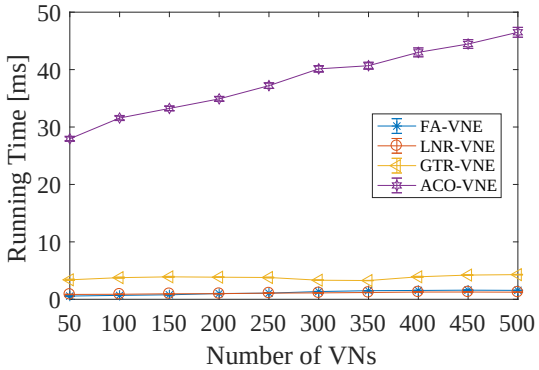

Fig. 13. Average Running Time for USNET

request is around 0.8ms and 2ms. However, the average time of ACO-VNE is between 17.5ms to 27.5ms due to its higher complexity. Figure 9 shows that *R/C Ratio* of ACO-VNE is fluctuated around 60.9%, which has 10% improvement compared with other algorithms that produce 50.5% average R/C ratio.

Figures 10-14 show the obtained results for the USNET topology as a function of number of VNs. Similar to the NSFNET topology, the factor values of α and γ are set to 0.5 and β is set to 0.8. For total power consumption as shown in Fig. 10(a), the improvement ratio of ACO-VNE can achieve up to 60.4%, 30.2% and 28.7% compared with FA-VNE, LNR-VNE and GTR-VNE, respectively. ACO-VNE can reduce 11.8%-18.6% network power consumption P_{net} compared with other three algorithms as shown in Fig. 10(b). In Fig. 10(c), the reduction ratio of DC power consumption P_{dc} of ACO-VNE is up to 65.78%, 41.52% and 38.8% when compared with FA-VNE, LNR-VNE and GTR-VNE, respectively. In addition, as shown in Fig. 11, the *Active DC Number* for ACO-VNE increases from 8 to 12 along with the increase of requests.

As shown in Fig. 12, the *Acceptance Ratio* of GTR-VNE and FA-VNE is 0.5% lower than ACO-VNE when the number of VNs is set to 500. However, the *Acceptance Ratio* of LNR-VNE is 97.1% which is 9.2% lower than ACO-VNE. The reason is that LTR node ranking just considers the resource utilization of the node itself. Therefore, the path between two higher ranking value nodes may not satisfy the requirement of virtual link. The *Running Time* of FA-VNE/LNR-VNE and GTR-VNE is around 0.8ms and 2ms respectively as shown in Fig. 13. However, the *Running Time* of ACO-VNE for each request is between 27.9ms to 46.5ms, which is 10ms more than the time under NSFNET as shown in Fig. 8. Figure 14 shows the *R/C Ratio* of ACO-VNE is dropped from 54.4% to 48.5% with the increase of VN requests. This is because mapping a virtual link will cause higher cost by allocating more substrate links to satisfy the request compared with NSFNET topology. For GTR-VNE and LNR-VNE, it is dropped from 41.99% and 48.46% to around 36.3%. The *R/C Ratio* of FA-VNE is around

36.5%.

To further evaluate the algorithms, the impact of GTR factor α under NSFNET is discussed as shown in Figs. 15-16. In Fig. 15, the *Acceptance Ratio* of ACO-VNE is 99.3% when α=0.3, while when α=0.5/0.7, the *Acceptance Ratio* is 99.5%. In addition, the *Acceptance Ratio* of GTR-VNE drops from 98.8% to 92.9% for α=0.7 when the number of requests increases from 400 to 500. For ACO-VNE, the *Active DC Number* is increased from 7 to 11 for any α value as shown in Fig. 16. However, for GTR-VNE, the range of *Active DC number* is [9,13] when α=0.7. For total power consumption, the results are similar with that is shown in Fig. 5. Therefore, the value of α has little influence on the performance of GTR in total.

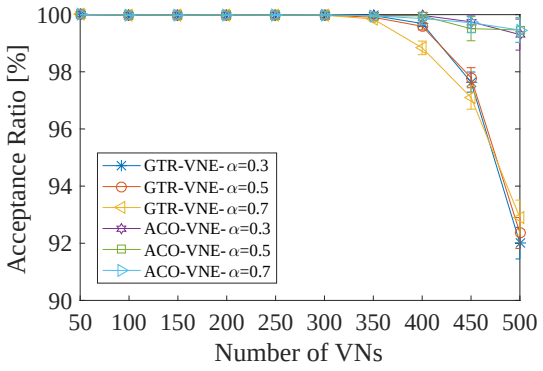

Fig. 15. Acceptance Ratio comparison for GTR α

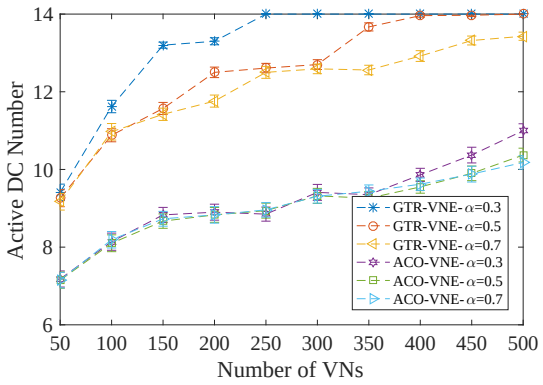

Fig. 16. Active DC Number comparison for GTR α

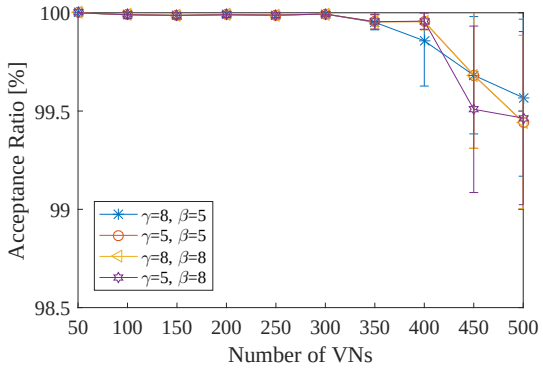

Fig. 17. Acceptance Ratio comparison for ACO γ and β

The impact of ACO factor γ and β under NSFNET is shown in Fig. 17. The *Acceptance Ratio* is greater than 99% for different setting of ACO factors. When the number of requests is more than 400, the margin of error for *Acceptance Ratio* has 0.5% increase, and the differences of average *Acceptance Ratio* are up to 0.1% among scenarios of ACO factors.

VII. Conclusion

VNE is one of the major challenges in network virtualization. Efficient VNE algorithms play an important role in reducing total power consumption, and increasing the acceptance ratio of VN requests and R/C ratio. In this paper, we have investigated location aware energy efficient VNE in SD-ODCNs. We formulated a MILP model to minimize total power consumption for VNE in SD-ODCNs. To reflect the selection possibility of each physical node for embedding virtual nodes, GTR node ranking method is proposed with considering both status of this node and its neighbors. Based on GTR, proposed GTR-VNE has proved that GTR is an efficient node ranking method which can obtain 5% increase of acceptance ratio compared with benchmarks. The simulation results show that proposed GTR-VNE outperforms the benchmarks in terms of power consumption and R/C ratio. In addition, based on artificial intelligence, proposed ACO-VNE algorithm has further improved the performance compared with GTR-VNE. Compared with GTR-VNE, total power consumption has been reduced by 18.8% and 28.7% for NSFNET and USNET, respectively. Furthermore, acceptance ratio and R/C ratio have been improved by ACO-VNE. The comparison results of GTR factor α and ACO factors γ and β show slight influence on the performance of ACO-VNE.

Acknowledgment

The authors would like to thank National Natural Science Foundation of China NSFC (61471109 and 61501104), Fundamental Research Funds for the Central Universities (N150406001, N150401002 and N161608001) and China Scholarship Council to support this work.

References

[1] N. M. M. K. Chowdhury and R. Boutaba, "A survey of network virtualization," *Comput. Netw.*, vol. 54, no. 5, pp. 862–876, 2010.

[2] N. M. M. K. Chowdhury and R. Boutaba, "Network virtualization: state of the art and research challenges," *IEEE Commun. Mag.*, vol. 47, no. 7, pp. 20–26, 2009.

[3] A. Fischer, J. F. Botero, M. T. Beck *et al.*, "Virtual network embedding: a survey," *IEEE Commun. Surv. Tutorials*, vol. 15, no. 4, pp. 1888–1906, 2013.

[4] A. Hammad, R. Nejabati, and D. Simeonidou, "Cross-layer optimization of network resource virtualization in IP over O-OFDM networks," *J. Opt. Commun. Netw.*, vol. 8, no. 10, pp. 765–776, 2016.

[5] L. Gong, H. Jiang, Y. Wang, and Z. Zhu, "Novel location-constrained virtual network embedding lc-vne algorithms towards integrated node and link mapping," *IEEE/ACM Transactions on Networking*, vol. 24, no. 6, pp. 3648–3661, December 2016.

[6] N. M. M. K. Chowdhury, M. R. Rahman, and R. Boutaba, "Virtual network embedding with coordinated node and link mapping," *INFOCOM*, pp. 783–791, 2009.

[7] W. Hou, Z. Ning, L. Guo, Z. Chen, and M. S. Obaidat, "Novel framework of risk-aware virtual network embedding in optical data center networks," *IEEE Systems Journal*, vol. PP, no. 99, pp. 1–10, 2017.

[8] W. Hou, Z. Ning, and L. Guo, "Green survivable collaborative edge computing in smart cities," *IEEE Transactions on Industrial Informatics*, vol. PP, no. 99, pp. 1–1, 2018.

[9] Z. Zhang, S. Su, K. Shuang, W. Li, and M. A. Zia, "Energy aware virtual network migration," in *2016 IEEE Global Communications Conference (GLOBECOM)*, Dec 2016, pp. 1–6.

[10] H. M. M. Ali, T. E. H. El-Gorashi, A. Q. Lawey, and J. M. H. Elmirghani, "Future energy efficient data centers with disaggregated servers," *Journal of Lightwave Technology*, vol. 35, no. 24, pp. 5361–5380, Dec 2017.
[11] L. Nonde, T. E. H. El-gorashi, and J. M. H. Elmirghani, "Energy efficient virtual network embedding for cloud networks," *J. Light. Technol.*, vol. 33, no. 9, pp. 1828–1849, 2015.
[12] S. Peng, R. Nejabati, and D. Simeonidou, "Role of optical network virtualization in cloud computing [invited]," *J. Opt. Commun. Netw.*, vol. 5, no. 10, pp. A162–A170, 2013.
[13] S. Gringeri, N. Bitar, and T. Xia, "Extending software defined network principles to include optical transport," *IEEE Commun. Mag.*, vol. 51, no. 3, pp. 32–40, 2013.
[14] D. Mcdysan, "Software defined networking opportunities for transport," *IEEE Commun. Mag.*, vol. 51, no. 3, pp. 28–31, 2013.
[15] G. M. Saridis, S. Peng, Y. Yan *et al.*, "Lightness: a function-virtualizable software defined data center network with all-optical circuit/packet switching," *J. Light. Technol.*, vol. 34, no. 7, pp. 1618–1627, 2016.
[16] C. Jackson, R. Nejabati, and F. o. Agraz, "Demonstration of the benefits of SDN technology for all-optical data centre virtualisation," in *Opt. Fiber Commun. Conf.*, 2017, pp. 3–4.
[17] Y. Ou, S. Yan, A. Hammad *et al.*, "Demonstration of virtualizeable and software-defined optical transceiver," *J. Light. Technol.*, vol. 34, no. 8, pp. 1916–1924, 2016.
[18] H. Yang, J. Zhang, Y. Zhao *et al.*, "SUDOI: software defined networking for ubiquitous data center optical interconnection," *IEEE Commun. Mag.*, vol. 54, no. 2, pp. 86–95, 2016.
[19] S. Peng, B. Guo, C. Jackson *et al.*, "Multi-tenant software-defined hybrid optical switched data centre," *J. Light. Technol.*, vol. 33, no. 15, pp. 3224–3233, 2015.
[20] P. Samadi, K. Wen, J. Xu *et al.*, "Software-defined optical network for metro-scale geographically distributed data centers," *Opt. Express*, vol. 24, no. 11, pp. 12 310–12 320, 2016.
[21] W. Van Heddeghem, B. Lannoo, D. Colle *et al.*, "A quantitative survey of the power saving potential in IP-over-WDM backbone networks," *IEEE Commun. Surv. Tutorials*, vol. 18, no. 1, pp. 706–731, 2016.
[22] F. Idzikowski, L. Chiaraviglio, A. Cianfrani *et al.*, "A survey on energy-aware design and operation of core networks," *IEEE Commun. Surv. Tutorials*, vol. 18, no. 2, pp. 1453–1499, 2016.
[23] M. N. Dharmaweera, R. Parthiban, and Y. A. Şekercioğlu, "Toward a power-efficient backbone network: the state of research," *IEEE Commun. Surv. Tutorials*, vol. 17, no. 1, pp. 198–227, 2015.
[24] G. A. Beletsioti, G. I. Papadimitriou, and P. Nicopolitidis, "Energy-aware algorithms for IP over WDM optical networks," *J. Light. Technol.*, vol. 34, no. 11, pp. 2856–2866, 2016.
[25] C. Lee and J. K. Rhee, "Traffic grooming for IP-over-WDM networks: energy and delay perspectives," *J. Opt. Commun. Netw.*, vol. 6, no. 2, pp. 96–103, 2014.
[26] P. Melidis, P. Nicopolitidis, and G. Papadimitriou, "Dynamic threshold reconfiguration mechanisms for green IP-over-WDM networks," *J. Light. Technol.*, vol. 34, no. 18, pp. 4354–4363, 2016.
[27] A. Shehabi, S. Smith, D. Sartor *et al.*, "United states data center energy usage report," 2016.
[28] M. Dayarathna, Y. Wen, and R. Fan, "Data center energy consumption modeling: a survey," *IEEE Commun. Surv. Tutorials*, vol. 18, no. 1, pp. 732–794, 2016.
[29] A. Hammadi and L. Mhamdi, "A survey on architectures and energy efficiency in data center networks," *Comput. Commun.*, vol. 40, pp. 1–21, 2014.
[30] S. Yang, P. Wieder, R. Yahyapour *et al.*, "Energy-aware provisioning in optical cloud networks," *Comput. Netw.*, vol. 118, pp. 78–95, 2017.
[31] M. Yuy, Y. Yiz, J. Rexfordy *et al.*, "Rethinking virtual network embedding : substrate support for path splitting and migration," *ACM SIGCOMM Comput. Commun. Rev.*, vol. 38, no. 2, 2008.
[32] X. Cheng, S. Su, Z. Zhang *et al.*, "Virtual network embedding through topology-aware node ranking," *ACM SIGCOMM Comput. Commun. Rev.*, vol. 41, no. 2, p. 38, 2011.
[33] S. Zhang, Z. Qian, J. Wu, and S. Lu, "An opportunistic resource sharing and topology-aware mapping framework for virtual networks," in *2012 Proceedings IEEE INFOCOM*, March 2012, pp. 2408–2416.
[34] L. Gong, Y. Wen, Z. Zhu *et al.*, "Toward profit-seeking virtual network embedding algorithm via global resource capacity," in *Proc. IEEE INFOCOM*, 2014, pp. 1–9.
[35] M. Chowdhury, M. R. Rahman, and R. Boutaba, "ViNEYard: virtual network embedding algorithms with coordinated node and link mapping," *IEEE/ACM Trans. Netw.*, vol. 20, no. 1, pp. 206–219, 2012.
[36] A. Hammad, R. Nejabati, and D. Simeonidou, "Novel methods for virtual network composition," *Comput. Netw.*, vol. 67, pp. 14–25, 2014.
[37] X. Guan, X. Wan, B. Choi *et al.*, "Ant colony optimization based energy efficient virtual network embedding," in *Int. Conf. Cloud Netw.*, 2015, pp. 273–278.
[38] W. Cao, H. Wang, and L. Liu, *An ant colony optimization algorithm for virtual network embedding*. Springer International Publishing, 2014, pp. 299–309.
[39] X. L. Chang, X. M. Mi, and J. K. Muppala, "Performance evaluation of artificial intelligence algorithms for virtual network embedding," *Eng. Appl. Artif. Intell.*, vol. 26, no. 10, pp. 2540–2550, 2013.
[40] M. Melo, S. Sargento, U. Killat *et al.*, "Optimal virtual network embedding: energy aware formulation," *Comput. Netw.*, vol. 91, pp. 184–195, 2015.
[41] S. Su, Z. Zhang, A. Liu *et al.*, "Energy-aware virtual network embedding," *IEEE/ACM Trans. Netw.*, vol. 22, no. 5, pp. 1607–1620, 2014.
[42] D. Chitimalla, K. Kondepu, L. Valcarenghi *et al.*, "5G fronthaul latency and jitter studies of CPRI over Ethernet," *J. Opt. Commun. Netw.*, vol. 9, no. 2, p. 172, 2017.